**Carcinogenesis** vol.34 no.6 pp.1382–1392, 2013
doi:10.1093/carcin/bgt041
*Advance Access publication February 6, 2013*

# Kif3a is necessary for initiation and maintenance of medulloblastoma

**Monique T.Barakat[1,2], Eric W.Humke[1,3,4] and Matthew P.Scott[1,*]**

[1]Departments of Developmental Biology, Genetics, and Bioengineering, [2]Medical Scientist Training Program, Program in Neurosciences and [3]Departments of Biochemistry and Medical Oncology, Howard Hughes Medical Institute, Stanford University School of Medicine, Clark Center West W252, 318 Campus Drive, Stanford, CA 94305-5439, USA

[4]Present address: Early Clinical Development, Genentech, Inc., 1 DNA Way, MS 442A, South San Francisco, CA 94080, USA

*To whom correspondence should be addressed. Email: mscott@stanford.edu

**Medulloblastoma (MB) cells arise from granule neuron precursors (GNPs) that have lost growth control. During normal development, GNPs divide in response to Sonic hedgehog (SHH), a ligand that binds to the patched (PTCH) receptor on GNPs. If one copy of the *Ptch* gene is lost, as in human Gorlin's syndrome and in *Ptch*$^{+/-}$ mice, MBs may form. Proper transduction of the SHH signal critically depends on primary cilia. Loss of primary cilia results in improper signal reception and failure to properly activate SHH target genes. KIF3a, part of a kinesin motor, is required for formation of primary cilia. Here, we use tamoxifen-induced ablation of *Kif3a* in GNPs of postnatal *Ptch*$^{+/-}$ mouse cerebella to show that KIF3a is necessary for MB formation. To investigate the importance of primary cilia in established tumors, we deleted *Kif3a* from cultured cells and from tumor cell grafts. The loss of *Kif3a* from established tumors led to their growth arrest and regression. MBs behave as if they are addicted to the presence of primary cilia. These results underscore the potential utility of agents that disrupt cilia for the treatment of Hh pathway-related MBs.**

## Introduction

The Hh pathway is critical for cell proliferation and morphogenesis at many stages of embryogenesis and postnatal development (1,2). In addition to the importance of Hh signaling in development, Hh signal transduction is disrupted in many types of cancer (3). A genetic screen for genes functioning in mouse gastrulation revealed that mutations in several genes necessary for primary cilium formation, transport and function are associated with mouse phenotypes suggestive of deficient Sonic hedgehog (SHH) signaling (4). Several Hh transduction proteins are localized within primary cilia, so these results together with the genetic data support a view of primary cilia as transduction centers for Hh signaling.

In the absence of a Hh ligand, PTCH receptor localizes in cilia of NIH3T3 cells (5). When SHH binds to PTCH, PTCH disappears from the cilia, enabling the seven transmembrane-domain protein SMOOTHENED (SMO) to enter cilia (6). SMO inhibits the function of the protein SUFU, which in turn controls the processing and/or transport of GLI transcription factors. SUFU and the three types of GLI protein (GLI1–3) are readily detected at distal tips of cilia (7). After Hh inactivates PTCH and causes SMO to move into cilia, a SMO-triggered change in GLI processing allows movement of activating forms of GLI proteins into the nucleus, where they induce transcription of target genes (5,6,8). Although most or all of the Hh pathway components are present in cilia, most are present and at least some are functional in other parts of the cell (9,10). For this reason, it is possible that some Hh transduction occurs outside cilia.

Primary cilia are cell cycle phase-specific organelles that extend from the maternal centriole. They frequently act as sensors of mechanical and chemical signals (11). Growing cells have primary cilia during S-phase, but disassemble the appendage prior to each cell division. In $G_2$ and M phases, cilium shortening occurs, leading to eventual cilium resorption or release from the plasma membrane (12). Cells exiting the cell cycle form new cilia. Ciliogenesis and cilium maintenance rely upon transport of axoneme assembly components to the extending tip of the cilium. This intraflagellar transport (IFT) requires motor and adaptor proteins for trafficking in anterograde (toward the tip or positive microtubule end) and retrograde (toward the negative microtubule end) directions. Cilium components and signal transduction proteins are transported as parts of multimeric protein complexes called IFT particles (13). KINESIN-2, which is a complex of KIF3a, KIF3b and KINESIN-2-associated proteins, moves IFT particles and their protein cargoes along the axoneme toward the ciliary tip (13). Mutations in *Kif3a* block Hh signal transduction during normal development (14). In the present study, we analyzed the effect of *Kif3a* mutation on initiation and maintenance of Hh pathway-driven cerebellar tumors.

SHH controls cell division in the mouse cerebellum. Granule neuron precursors (GNPs) in the external germinal layer of the cerebellum proliferate (15), stimulated by SHH transmitted by Purkinje neurons (16–18). The newly formed granule neurons extend axons that synapse with Purkinje cell dendrites in the molecular layer, whereas granule neuron cell bodies migrate from the external germinal layer through the layer containing Purkinje cell bodies to the internal granule layer (15). The buildup of PTCH in GNPs in response to SHH may restrain ongoing SHH signaling by binding ligand and by inhibiting SMO, perhaps contributing to the cessation of GNP production that normally occurs in mice about 2 weeks after birth. In keeping with that idea, loss of restraining Hh pathway proteins such as SUFU or PTCH can lead to medulloblastoma (MB), a cancer arising from unrestrained growth of GNPs that is the most common malignant childhood brain tumor.

MBs have multiple causes including altered Hh or Wnt signaling (19). The initial identification of damage to the Hh pathway as a cause of MB arose when mutations in human *PTCH* were discovered to cause Gorlin's syndrome, a birth defects syndrome with associated high rates of MB (20,21). When growth restraint by PTCH is genetically reduced, as in the *Ptch*$^{+/-}$ mouse model of Gorlin's syndrome, some GNPs continue to proliferate beyond the usual time. The consequence can be formation of preneoplastic lesions and MB (22). The importance of Hh target genes for MBs is also supported by the inhibition of MB growth that occurs when Hh signal transduction is blocked by cyclopamine (23). In humans, MB formation appears to occur over the course of years, probably beginning with a mutant GNP during cerebellum development (birth to 1 year of age), and typically leading to symptomatic MB at about 7 years of age (24). In mice predisposed to spontaneous tumorigenesis, such as *Ptch*$^{+/-}$ heterozygous mice, formation of tumors including MB occurs in some mice within the first months of life (22).

The discovery of the importance of primary cilia for Hh signal transduction led to the discovery that cilia are important for early stages of cerebellum development (25,26). Pioneering ultrastructure studies of MBs identified primary cilia on their cell surfaces as well (27). Mouse models of MB used to investigate the role of cilia in tumor initiation have given complex results. Cilia are required for growth of tumor cells that have constitutive Hh target gene transcription due to hyperactive SMO, but cilia restrain growth of tumor cells when target gene activation occurs in response to a mutant *Gli2* (28).

Among the several mouse models of MB, only one, *Ptch* heterozygous mice, has the same genetic cause as Gorlin syndrome (22). Here,

**Abbreviations:** ER, estrogen receptor; GNP, granule neuron precursor; H&E, hematoxylin and eosin; IFT, intraflagellar transport; MB, medulloblastoma; MTT, 3-(4,5-dimethylthiazole-2-yl)-2,5-diphenyl tetrazolium bromide; SAG, Smoothened Agonist; SHH, Sonic hedgehog; SMO, SMOOTHENED.

we investigate the role of *Kif3a* in tumorigenesis in these mice. We deleted *Kif3a* from the GNP cells, the cell type of origin for spontaneous MB. Cultured MB cells and an allograft mouse model of MB were used to probe the role of KIF3a in growing tumor cells and in established tumors. In this way, we tested whether interference with cilia formation can arrest or reverse tumors that had already started to grow, a situation analogous to newly diagnosed human MB patients.

## Materials and methods

### *MB cell line derivation*

MB cell lines were produced using an adapted serial dissociation protocol (29) modified to include an initial serum-free neurobasal medium culture for 2 days followed by 24 h serial dissociation of MB tissue using collagenase, dispase and hyaluronidase. Immortalization was carried out by serial passaging and confirmation of stable Shh pathway target gene expression after every fifth passage. Cell lines were deemed immortalized after 25 passages.

### *Cell culture*

GNP preparation and culture was carried out as described previously (16). For *Kif3a* ablation in fibroblasts, *Kif3a*$^{fl/fl}$ MEFs were derived in our laboratory from a mouse engineered to have loxP sites surrounding the *Kif3a* gene. A Cre recombinase fused to a modified estrogen receptor (ER) was then delivered into the cell line by retroviral infection. For ciliation studies, cells were treated as described previously (5) except the MB cell lines were starved in 0% fetal bovine serum. Cells were transfected with Gli2-Flag construct (obtained from C.C.Hui) using Lipofectamine 2000 (Invitrogen) per the manufacturer's provided instructions. *In vitro* tamoxifen treatment was carried out using 4-OH tamoxifen (CalBiochem). The PZP53 MB cell line was obtained from P.Beachy (23). The mouse colon carcinoma cell line CT26 was obtained from ATCC (CRL2638).

### *Antibodies*

Anti-p38 and anti-Kif3a were purchased from Abcam (ab7952, ab11259), anti-Gli1 from Cell Signaling Technologies (L42B10), anti-acetylated tubulin from Sigma (T6793) and Hoechst/DAPI stain from Sigma (D9542). Secondary antibodies conjugated to horseradish peroxidase were from Jackson Laboratories. Anti-Ptch1 rabbit polyclonal antibody and anti-Smo rabbit polyclonal antibodies have been described (5). Standard hematoxylin and eosin (H&E) staining was used for tissue samples. Microscopy was performed using a Leica (DMIL) brightfield photomicroscope and a Leica confocal microscope (Leica DMIRE2). Images were assembled using Adobe Photoshop CS4 and brightness/contrast were adjusted for optimal viewing; any manipulation was applied to the entire image.

### *Quantitative PCR*

Cellular RNA was isolated using Trizol (Invitrogen). cDNA was prepared using SuperScript III First Strand Kit (Invitrogen). Real-time (quantitative) PCR (Bio-Rad) was used to measure and quantify transcript levels. TaqMan (Applied Biosystems) gene expression probes used were Mm00970977_m1 (*ptch1*), Mm00494645_m1 (*gli1*), Mm00257977_m1 (*gli2*) and Mm99999915_g1 (*gapdh* for establishment of baseline).

### *Cell lysate preparation and western blot analysis*

For the production of whole-cell, cerebellum and GNP lysates, cells were lysed in 50 mM Tris at pH 7.4, 300 mM NaCl, 2% NP-40 (v/v), 0.25% deoxycholate (w/v), 10 mM *N*-ethyl maleimide, 1 mM dithiothreitol and protease inhibitor cocktail (ethylenediaminetetraacetic acid-free, Roche).

### *Mice*

All mouse procedures were approved by the Stanford International Animal Care and Use Committee (APLAC Protocol 10424, 10412). Genetically modified mice *Ptch*$^{+/-}$ (108B2 line) were generated in our laboratory (22); 4–6-week-old *Nude*/*Nude* mice were obtained from Charles River Labs; other mice were obtained from laboratories listed in the indicated references: *Kif3a*$^{fl/fl}$ (30) and *Math1-Cre*$^{ER}$ (31). For genotyping, ear clips and/or tail clips were digested in Proteinase K (Invitrogen)-containing buffer; 2 µl was used to run PCR (38 cycles of 95°C for 30 s denaturing, 52°C for 30 s annealing, 70°C for extension).

Induction of Cre recombinase activity in GNPs in the cerebellum was accomplished by administration of tamoxifen (32). Tamoxifen (Sigma) was dissolved in corn oil (Sigma) at 5 mg/ml at 37°C, filter sterilized and stored for up to 7 days at 4°C in the dark. A gavage syringe appropriate to mouse esophageal size was used to administer tamoxifen to pups at a dose of 3–4 mg/40 g body weight (calculated based on the average pup size) on postnatal days 1 and 4. Tamoxifen was administered to adult nude mice at a dose of 8 mg/40 g body weight. An equivalent volume of sterile filtered corn oil alone was used for vehicle treatment groups.

### *Tumorigenesis and cell survival assays*

Nude mice received cell injections: 800 000 cells per flank or shoulder for the experiment documented in Figure 2 ($n = 6$) and 1.6 million cells per flank or shoulder for all other heterotopic tumor assays ($n = 8$). Following injection, cells were incubated with 1 ml propidium iodide (Sigma; 50 µg/ml in phosphate-buffered saline) and survival was consistently >85%. Tumor size was measured every 3 days with a digital caliper and tumor diameter was calculated using the standard modified ellipse formula ($0.5 \times \text{length} \times \text{width}^2$). Orthotopic tumor allografts were carried out using a stereotactic injection system. Forty thousand MB cells in 5 µl phosphate-buffered saline were injected into the central cerebellum. Soft agar transformation assay was performed in 6 cm plates, and $5 \times 10^4$ cells were added to 3 ml 0.3% LMP agarose (Sigma) with 15% serum + Dulbecco's modified Eagle's medium and plated on top of solidified 0.5% LMP agarose with 15% serum + Dulbecco's modified Eagle's medium. After 18 days, colonies larger than 2 mm were counted. Cell growth rate was determined using the 3-(4,5-dimethylthiazole-2-yl)-2,5-diphenyl tetrazolium bromide (MTT) survival assay (33). Results of the assay are reported as 'cell growth ratio', a standard normalized optical density value that corrects for absorbance and is reported relative to a single cell type (which is assigned a growth ratio of one). For the MTT assay, cells ($3 \times 10^3$/well) were plated in 96-well culture plates. Survival was assessed at indicated time points by the addition of 20 µl MTT and incubation for 2 h; absorbance was measured at 570 nm.

## Results

### *Kif3a is necessary for MB tumor initiation*

We designed experiments to assess the importance of *Kif3a* in malignant transformation of GNPs to MB. GNPs, and MB arising from them, characteristically express *Math1*, which encodes a basic helix–loop–helix transcription factor. A *Math1* enhancer directing expression of reporter genes in a *Math1*-specific pattern was reported previously (34). *Math1* expression is restricted to GNPs in the developing cerebellum, with loss of expression upon differentiation into granule neurons (35). By 2 weeks after birth, mouse pups have little to no detectable *Math1* RNA or *Math1*-driven GFP in the cerebellum. We performed crosses to generate mice with a *Math1* enhancer directing production of Cre$^{ER}$ recombinase in *Kif3a*$^{fl/fl}$, *Ptch*$^{+/-}$ GNPs. Tamoxifen was administered to *Ptch*$^{+/-}$, *Math1-Cre*$^{ER}$, *Kif3a*$^{fl/fl}$ mice on postnatal days 1 and 4 to trigger ablation of *Kif3a* in postnatal GNPs (Figure 1A and B) and remove *Kif3a* transcripts (Figure 1C) and protein (Figure 1D) from GNPs. KIF3a protein became undetectable in granule neurons, but other cells in the cerebellum, including Purkinje cells, ependymal cells, leptomeningeal cells and glia, still had normal KIF3a levels (Figure 1E).

Mature GNs in tamoxifen-treated *Math1-Cre*$^{ER}$ *Kif3a*$^{fl/fl}$ mice had substantially fewer cilia than *Math1-Cre*$^{ER}$ *Kif3a*$^{fl/fl}$ GNs not treated with tamoxifen (Supplementary Figure 1A, available at *Carcinogenesis* Online). GNPs from tamoxifen-treated *Math1-Cre*$^{ER}$ *Kif3a*$^{fl/fl}$ mice had a similar decrease in cilia 10 days after initial tamoxifen treatment (Supplementary Figure 1B, available at *Carcinogenesis* Online). Residual KIF3a protein present in GNPs in adult *Cre*$^{ER}$, *Kif3a*$^{fl/fl}$ mouse cerebella (Figure 1E) was sufficient to sustain apparently normal cerebellum development (Figure 1F). Cerebella from mice with *Kif3a*-deficient GNPs were morphologically and histologically indistinguishable from controls. In contrast, mice constitutively lacking KIF3a protein in all *hGFAP*-expressing cells have severely impaired cerebellum development (28).

Tamoxifen-treated *Math1-Cre*$^{ER}$ *Kif3a*$^{fl/fl}$ *Ptch*$^{+/-}$ mice never developed MB (0 MB/126 mice) (Figure 1G, red line). Tamoxifen did not have a global antitumor effect because mice with *Kif3a*-deficient GNPs still produced rhabdomyosarcomas at the expected rate (11%). Furthermore, treatment of *Math1-Cre*$^{ER}$ *Ptch*$^{+/-}$ mice treated with tamoxifen developed tumors at a rate indistinguishable from *Ptch*$^{+/-}$ mice and *Math1-Cre*$^{ER}$ *Ptch*$^{+/-}$ mice that were not treated with tamoxifen. Control mice without the floxed *Kif3a* allele, treated with either tamoxifen or corn oil vehicle control, developed MBs and rhabdomyosarcomas at rates indistinguishable

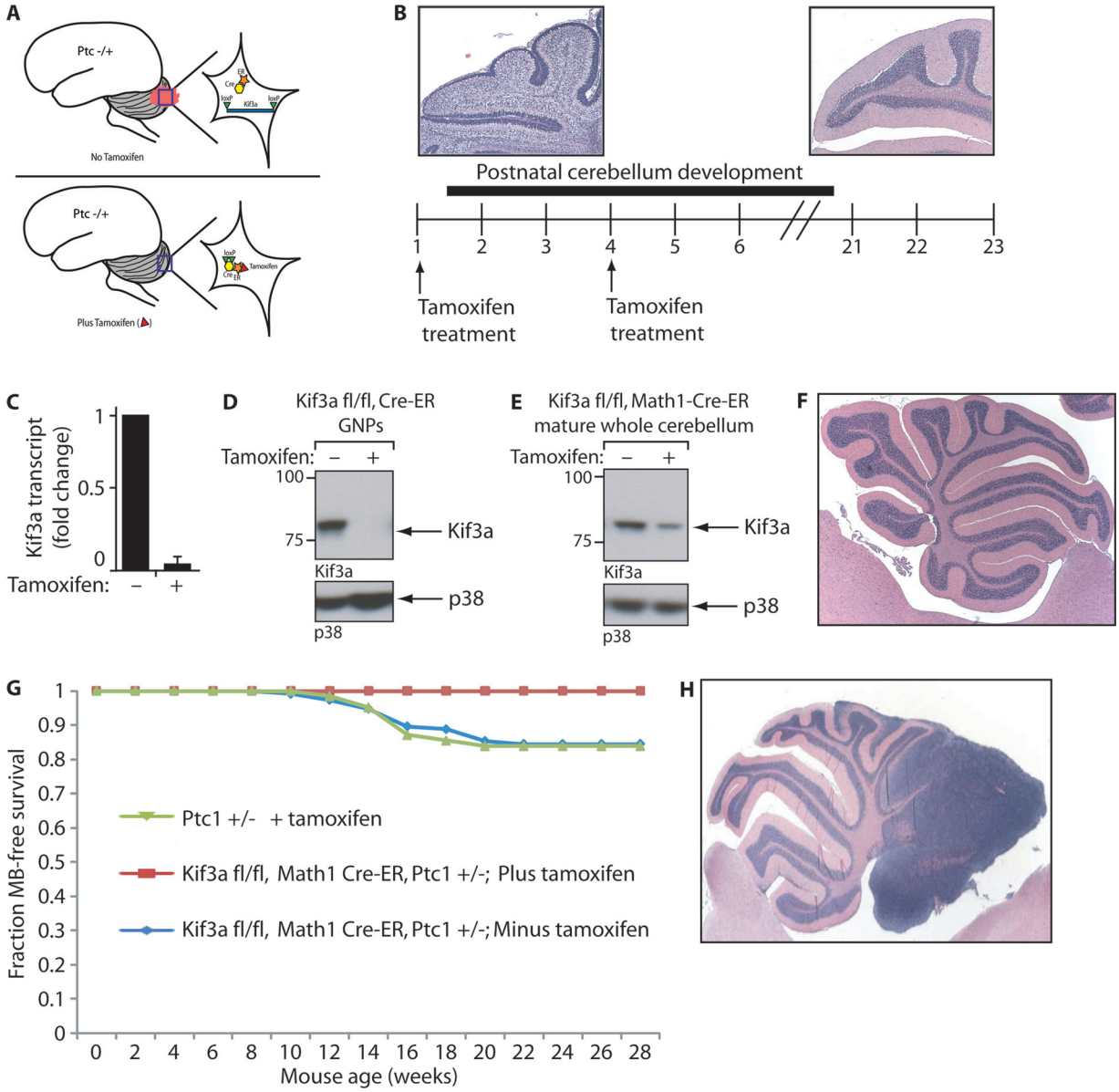


**Fig. 1.** *In vivo* mutation of *Kif3a* by postnatal administration of tamoxifen to *Math1-Cre*$^{ER}$, *Kif3a*$^{fl/fl}$, *Ptch*$^{+/-}$ mice prevents MB. (**A**) Schematic showing experimental design for deletion of *Kif3a* in GNPs. (**B**) Tamoxifen was administered to mice on postnatal days 1 and 4 to achieve optimal Cre$^{ER}$-mediated recombination and deletion of *Kif3a*. The postnatal cerebellum development period is indicated by black bar and H&E image of developing cerebellum is shown with GNPs in the external granule cell layer (upper left). A mature cerebellum, devoid of GNPs, is shown for comparison above timeline corresponding with a developed cerebellum (upper right). (**C**) Quantitative PCR showing that *Kif3a* transcript is minimal in GNPs at postnatal day 7. Error bars depict ±SE. (**D**) Protein blot of GNPs from vehicle-treated and tamoxifen-treated pups. Tamoxifen-treated pups have undetectable levels of KIF3a at postnatal day 10. (**E**) Protein blot of whole adult cerebellum from a mouse that was vehicle treated and one that was tamoxifen treated according to the protocol in (B). Reduced, but detectable levels of KIF3a are present. (**F**) H&E stain illustrating one cerebellum from an adult mouse that underwent tamoxifen treatment protocol depicted in (B). Cerebella from tamoxifen-treated mice showed normal development and morphology of the cerebellum. (**G**) MB survival curve showing that vehicle-treated control mice (blue line) and tamoxifen-treated *Ptch*$^{+/-}$ mice (green line) developed MB at the expected rate (17 MB/116 mice), within the anticipated time frame. In contrast, tamoxifen-treated *Kif3a*$^{fl/fl}$, *Math1 Cre-ER Ptch*$^{+/-}$ mice resulting in *Kif3a*-deficient GNPs (red line) did not develop MB (0 MB/126 mice). Error bars depict ±SD. (**H**) H&E stain showing an example of MB that developed in vehicle-treated mice. These tumors are histologically indistinguishable from those that occur in *Ptch*$^{+/-}$ mice.

from *Ptch*$^{+/-}$ mice (Figure 1G, green and blue lines). MB onset, volume, location, histology and Hh target gene expression profiles did not differ significantly between control *Math1-Cre*$^{ER}$ *Kif3a*$^{fl/fl}$ *Ptch*$^{+/-}$ and *Ptch*$^{+/-}$ mice (data not shown). We conclude that *Kif3a* function is necessary for MB formation in Gorlin's syndrome mice.

*Loss of Kif3a from cultured fibroblasts has no effect on their growth*

The inability to form MB in *Ptch*$^{+/-}$ mice lacking *Kif3a* in their GNP cells led us to ask whether loss of Kif3a has a general effect on cell growth. Fibroblasts derived from a *Kif3a*$^{fl/fl}$ Cre-ER mouse (36) were treated with tamoxifen to inactivate the *Kif3a* gene (Figure 2A–C). KIF3a protein is stable, taking ~8 days to reach minimal levels after tamoxifen treatment (Figure 2C). This time course of loss of Kif3a protein correlates with the time course of cilia disappearance. Primary cilia were rarely detected in cells after loss of Kif3a protein (Figure 2D) The growth characteristics of fibroblasts with or without tamoxifen was the same (Figure 2F). Therefore, KIF3a is dispensable for fibroblast growth in culture. We next tested whether the removal of KIF3a had any discernable effect on the fibroblasts by testing their ability to respond to Hh pathway agonists.

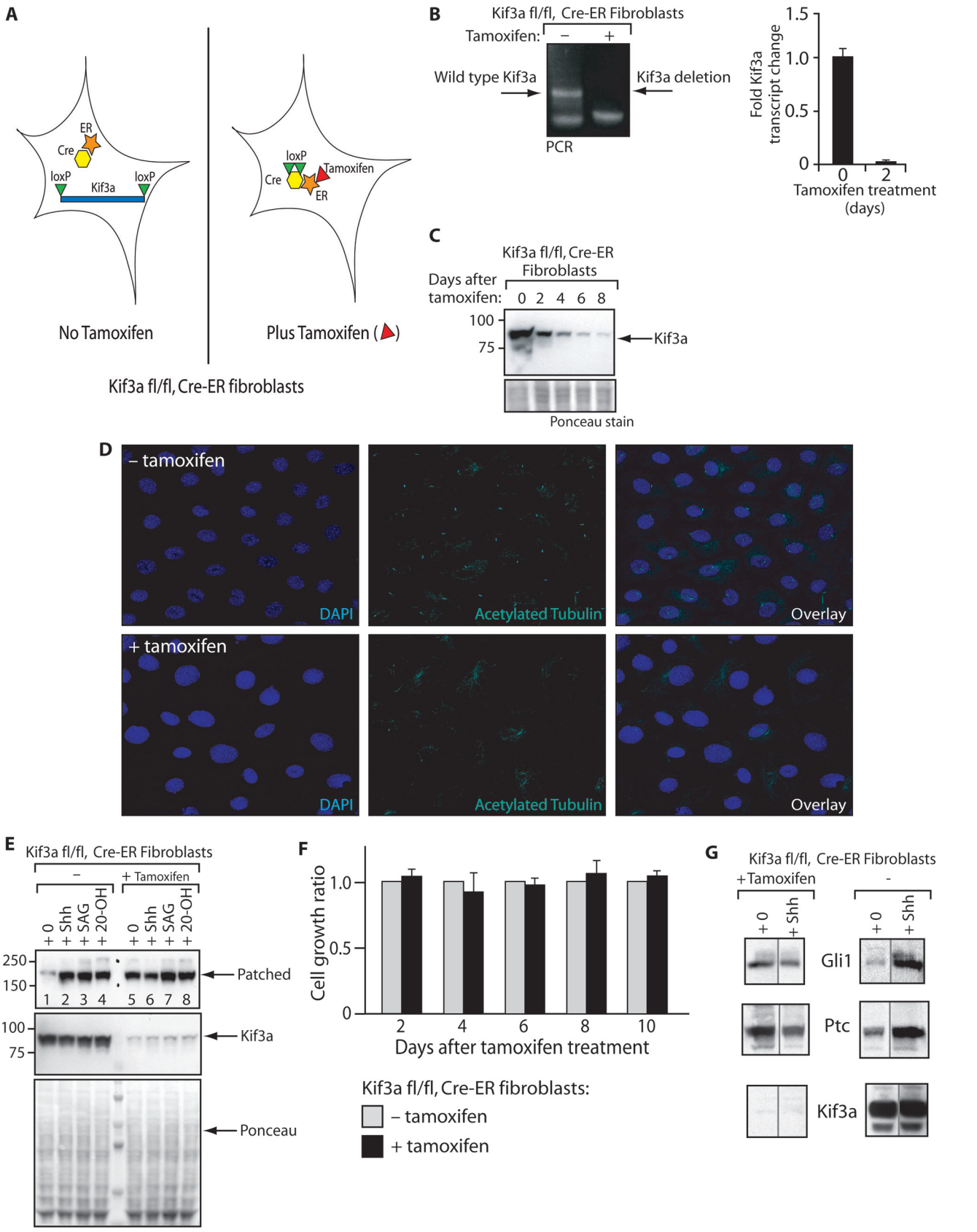


**Fig. 2.** A tamoxifen-treated $Cre^{ER}$, $Kif3a^{fl/fl}$ fibroblast cell line derived from $Kif3a^{fl/fl}$ mice has normal cell survival and proliferation, but loss of cilia and deficient Hh responsiveness. (**A**) Experimental schematic for tamoxifen-induced *Kif3a* deletion in fibroblasts. (**B**) Genomic PCR from $Kif3a^{fl/fl}$ $Cre^{ER}$ fibroblasts showing genomic deletion of *Kif3a* (absence of wild-type band) 1 day after tamoxifen treatment (left panel, right lane). Reverse transcription–polymerase chain reaction of *Kif3a* transcript level 2 days after tamoxifen treatment (right panel). Error bars depict ±SE. (**C**) Protein blot showing KIF3a protein, which does not reach minimum levels until 8 days following tamoxifen treatment and genomic deletion of *Kif3a*. (**D**) Confocal images (×20) after immunostaining to highlight nuclei

Stimulation of fibroblasts with the pathway agonists SHH, Smoothened Agonist (SAG) and 20-hydroxycholesterol (20-OH) normally induces numerous genes including *Ptch*. SHH induces pathway target gene expression by binding to the PTCH receptor. SAG and 20-OH stimulate pathway target gene expression by binding downstream of the PTCH receptor and act at or near the level of pathway signal transducer, Smoothened. The amount of PTCH serves as a measure of target gene activity (Figure 2E, lanes 1–4). Each agonist induced accumulation of PTCH to at least 10-fold more than the control. *Kif3a* deletion resulted in a higher level of PTCH in cells not treated with agonist, perhaps due to reduced negative regulation of Hh transduction (37) (Figure 2E, lane 5). Addition of SHH slightly lowered PTCH protein (Figure 2E, compare lane 5 with 6), whereas SAG, an agonist that acts directly on Smoothened, caused PTCH to accumulate only about 2-fold more than in the control (Figure 2E, lanes 7 and 8). 20-OH, another inducer, had a similar modest effect. GLI1 is another Hh pathway target gene and GLI1 protein levels follow a trend similar to PTCH protein levels in wild-type fibroblasts and fibroblasts treated with SHH agonist after Kif3a deletion (Figure 2G).

These data show that fibroblasts can proliferate normally in the absence of functional KIF3a, as has been reported previously for other cell lines (30,36), but fibroblasts lacking KIF3a have an impaired response to Hh pathway agonists.

### *Loss of Kif3a results in growth arrest of transformed MB cells*

Fibroblasts grow without KIF3a, but we show that Kif3a is necessary for initiation of MB, suggesting that these tumor cells are different. In cultured fibroblasts, SHH ligand stimulates transcription of target genes most effectively when cells are contact inhibited (confluent), nutrient restricted (serum deprived) and predominantly quiescent. Under these conditions >90% of NIH3T3 fibroblast-like cells are ciliated. In contrast, cultured MB cells derived from a $Ptch^{+/-}$ mouse MB tumor proliferated relentlessly in conditions of serum deprivation, ignoring contact inhibition and nutrient status cues. Fewer than 10% of cultured, confluent, $Ptch^{+/-}$ MB cells formed cilia when subjected to the standard 24 h serum-restriction protocol, which results in cilia formation in NIH3T3 cells (Figure 3A).

To determine the optimal length of time for formation of primary cilia in $Ptch^{+/-}$ MB cells, different times of serum starvation were tested. After 96 h of serum deprivation, 68% of MB cells formed cilia (Figure 3B). SMO protein became concentrated in ~59% of the primary cilia in cultured MB cells (Figure 3C), consistent with the high level of SHH target gene activity known to occur in MB tumors (22). Thus, MB cells in culture eventually form primary cilia, but do not ciliate as readily or under the same conditions as cultured NIH3T3 cells. These findings guided our studies of roles of cilia in a newly created MB cell line.

We derived a MB cultured cell line with tumorigenic potential from a $Ptch^{+/-}$ mouse tumor to see whether the cells require *Kif3a* for growth. The MB cell line, '$MB^{Kif\text{-}CreER}$', was genotypically *Math1-*$Cre^{ER}$, $Kif3a^{fl/fl}$, $Ptch^{+/-}$, enabling the deletion of *Kif3a* using *in vitro* tamoxifen treatment. After immortalization, the cells had a faster doubling time than fibroblasts (Figure 4A), similar to that of a murine colon carcinoma cell line (38). $MB^{Kif\text{-}CreER}$ cells were able to form cilia (Figure 4B and C) and formed colonies in soft agar (Figure 4D).

Anchorage-independent growth is one indicator of the metastatic potential of cells. $MB^{Kif\text{-}CreER}$ cells injected into the flanks (Figure 4E) or cerebella (Figure 4F) of immunodeficient nude mice formed solid tumors. Neuropathological analysis of the flank and cerebellar tumors revealed indistinguishable cytology, except that the cerebellar tumors infiltrated adjacent normal tissue. All the tumors had closely packed, enlarged, undifferentiated cells with high nuclear to cytoplasmic ratios, nuclear molding, frequent mitotic figures and focal necrosis, all features of embryonal central nervous system neoplasms. Immunohistochemistry showed focal GFAP protein accumulation in flank and cerebellar tumors, without detectable synaptophysin or β-catenin staining (Supplementary Figure 3A, available at *Carcinogenesis* Online). These features are diagnostic of MB.

We tested the role of KIF3a in MB cell survival by treating $MB^{Kif\text{-}CreER}$ cells with tamoxifen *in vitro*. In contrast to fibroblasts, MB cells required Kif3a for their survival in culture. $MB^{Kif\text{-}CreER}$ cells underwent growth arrest following tamoxifen treatment, at a time consistent with disappearance of KIF3a and cilia (Figure 5A).

### *Complementation by Gli2 overcomes MB growth arrest associated with the loss of Kif3a*

We tested whether the growth arrest of MB cells after inactivation of *Kif3a* and loss of primary cilia was dependent upon interference with the Hh pathway. The goal was to see whether other pathways that might be affected by *Kif3a* mutation. If the important effect was upon Hh transduction, it should be possible to rescue the cells by activating SHH target genes. To MB cells lacking *Kif3a*, we provided GLI2, the major Hh transcriptional activator, to see whether this would overcome the growth arrest. Transfection of *Gli2-FLAG* (39) at the time of tamoxifen treatment protected tamoxifen-treated $MB^{Kif3a\text{-}CreER}$ cells from cell death (Figure 5B). GLI2 levels were 4.5-fold higher compared with untransfected, tamoxifen-treated $MB^{Kif\text{-}CreER}$ cells (Figure 5C). Five days after tamoxifen treatment, when KIF3a levels were reduced, the $MB^{Kif\text{-}CreER}$ cells without added GLI2 had far less GLI1 protein (a SHH target) than control cells where KIF3a remained functional (Figure 5D). Signature transcriptional targets of the Wnt, TGF-β, AKT and PDGF signaling pathways were unchanged (Supplementary Figure 2B, available at *Carcinogenesis* Online). We conclude that the deaths of tamoxifen-treated $MB^{Kif\text{-}CreER}$ cells in the absence of added GLI2 was due to the lack of SHH target gene expression. Restoration of active GLI2, and consequently SHH target gene activity, eliminated the need for *Kif3a* in $MB^{Kif\text{-}CreER}$ cell survival.

### *Loss of Kif3a results in growth arrest of established MB tumors*

We used mouse allografts to learn how loss of KIF3a affects already-established MB tumors. Due to the time it takes for tamoxifen to reduce Kif3a protein levels compared with the rapid rate of growth of MB and consequential rapid mortality from intracranial MB, these experiments could only be done with flank tumors but not with intracranial tumors. This situation is akin to a newly diagnosed pediatric patient carrying a MB, in contrast to experiments described above that show KIF3a is required to form MBs. $MB^{Kif\text{-}CreER}$ cells were tested for their ability to exhibit anchorage-dependent growth by growing them in soft agar in the presence or absence of tamoxifen. Tamoxifen prevented the cells from forming colonies in soft agar (Figure 6A and B). To ensure that tamoxifen did not have a general toxic effect, murine colon cancer cells were treated with tamoxifen. They formed colonies at the same rate as untreated cells (Supplementary Figure 4A, available at *Carcinogenesis* Online). $MB^{Kif\text{-}CreER}$ cells treated *in vitro* with tamoxifen and injected into flanks and shoulders of immunodeficient mice did not form solid tumors (Figure 6C). A $Ptch^{+/-}$, $p53^{-/-}$ MB cell line (23) formed solid tumors at a similar rate with or without

←
(DAPI, blue) and cilia (acetylated tubulin, cyan). Abundant cilia are present in $Cre^{ER}$, $Kif3a^{fl/fl}$ fibroblasts (top panel), but only rarely are cilia seen 9 days after tamoxifen treatment. (**E**) Protein blot showing that with functional *Kif3a* the Hh pathway-stimulating inducers (SHH, SAG and 20-OH, which are thought to act at the level of Smoothened) cause accumulation of increased PTCH protein. In contrast, tamoxifen-treated cells lacking *Kif3a* have more modest increases in PTCH protein in response to the inducers (lanes 5–8). Ponceau stain of protein blot included to demonstrate equal loading of protein. (**F**) MTT survival assay showing that tamoxifen treatment and loss of *Kif3a* transcript and protein does not alter survival of $Cre^{ER}$, $Kif3a^{fl/fl}$ fibroblasts. Error bars depict ±SE. (**G**) Protein blot showing that SHH treatment leads to increased PTCH and GLI1 protein in cells with functional *Kif3a*. Tamoxifen-treated cells lacking *Kif3a*, in contrast, have higher levels of PTCH and GLI1 prior to SHH treatment and do not show a further increase in PTCH or GLI1 levels after SHH treatment. Protein levels were measured and normalized for loading.

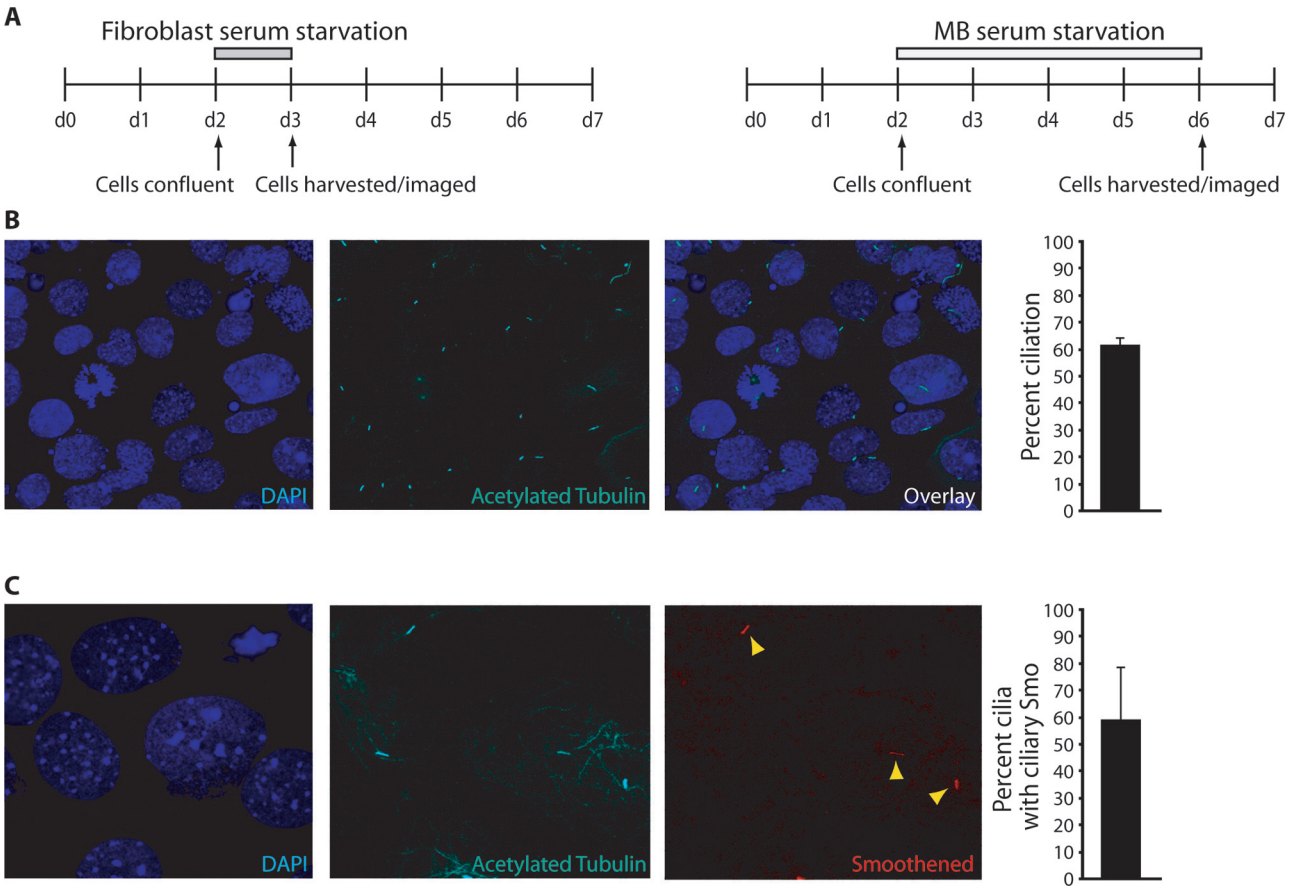


**Fig. 3.** Confluent *Ptch*$^{+/-}$ mouse MB cells form cilia after prolonged serum deprivation. (**A**) Schematic diagram of protocol to induce cilia formation in fibroblasts versus MB cells. Gray bars represent the duration of serum restriction (0.5% serum, fibroblasts) or serum starvation (0% serum, MB cells). (**B**) Cultured *Ptch*$^{+/-}$ MB cells with nuclei highlighted by DAPI stain (far left panel) have primary cilia highlighted by acetylated tubulin (middle panel). Overlay, far right panel. Bar graph on far right depicts MB cell percent ciliation (number of cilia/number of nuclei) quantified from three independent serum-deprivation experiments. Error bars depict ±SE. (**C**) Cultured *Ptch*$^{+/-}$ MB cells with nuclei highlighted by DAPI stain (far left panel) have primary cilia highlighted by acetylated tubulin (middle panel). Ciliary SMO is apparent in a subset of MB cells (red, far right panel). Bar graph depicts percentage of ciliated MB cells with ciliary SMO. Error bars depict ±SE.

the addition of tamoxifen (Supplementary Figure 4B, available at *Carcinogenesis* Online).

We treated already-established *Math-1*$^{CreER}$ *Kif3a*$^{fl/fl}$ flank tumors with either tamoxifen or vehicle control. Flank tumors treated with tamoxifen initially underwent growth arrest and then regressed over 30 days following treatment (Figure 6D). Vehicle-treated tumors continued to grow. In mice that underwent tamoxifen treatment, and consequently inactivation of *Kif3a* in *Math1*-expressing MB cells, flank tumors had necrotic tissue with lower cell density, interspersed with regions of necrosis and fibrosis (Figure 6E).

## Discussion

### *Primary cilia in cerebellum development and MB*

Among several mouse models of MB, only one has the same genetic lesion as human Gorlin syndrome, which is due to *PTCH* haploinsufficiency (22,40). The sequence and frequency of events in the human neoplastic transformation of a GNP to MB is preserved in the *Ptch*$^{+/-}$ heterozygous mouse model of MB. About 15% of mice that are heterozygous for a null *Ptch* mutation develop MB by 5 months of age (22,40). The tumors arise sporadically, spontaneously and focally in mice with a mature cerebellum and are histologically similar to human MB. *Ptch*$^{+/-}$ mice recapitulate the human Gorlin syndrome in that tumors occur in association with basal cell carcinoma and rhabdomyosarcoma (22). Non-Gorlin syndrome mouse models of Hh pathway-driven MB have been engineered to activate Hh targets in all GNPs by conditional loss-of-function of both alleles of *PTCH* (41) or by introducing an activating *Smo*$^{M2}$ or *Smo*$^{A2}$ allele (42). Tumors that develop in these other mouse models differ from each other and from human Gorlin syndrome-associated tumors. Both models rely upon tissue-specific drivers and result in unrestrained proliferation of GNPs, culminating by 2 months of age in extensive lesions that encase the cerebellum in 90–100% of mice (41,42). These genetic alterations, and the tumors that arise from them, do not represent the usual sequence of events that occurs in pediatric MB.

Han *et al.* (28) studied the need for *Kif3a* in central nervous system tumors, including MB, using an activated *Smo* allele or a GLI2 constitutively active (CA) model. Our findings are consistent with theirs in that Hh pathway-driven MBs do not develop without functional primary cilia. Their study employed conditional *Kif3a* mutant mice that express Cre recombinase controlled by the *hGFAP* driver, which stimulates recombination in GNPs, all neural stem cells, and many neurons and ependymal cells (43). Tumors that developed in the *Smo*$^{M2}$ mouse brains were highly malignant, encasing the majority of developing cerebellum folia by postnatal day 10 (28). Tumors that developed in *Gli2-CA* mice occurred much later in life, were distributed throughout the central nervous system and had high expression levels of Hh and WNT target genes (28). The authors concluded that cilia can either promote or inhibit Hh-driven brain tumors and basal cell carcinoma, depending on how the Hh pathway is activated, with tumor promotion occurring in the *Gli2-CA* model and tumor suppression occurring in the *Smo*$^{M2}$ model (28,44).

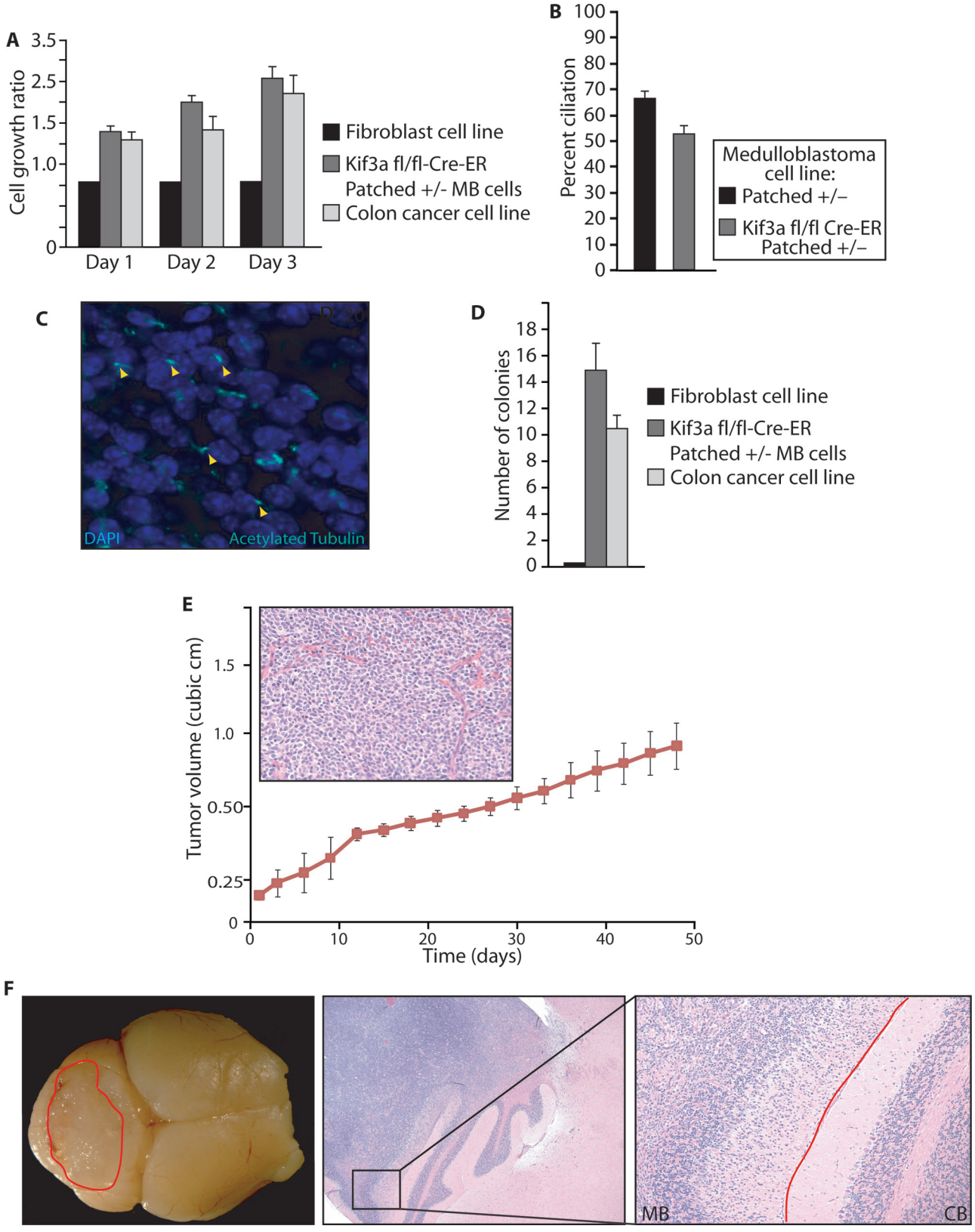


**Fig. 4.** *In vitro* MB cell line derived from *Kif3a Math1-Cre$^{ER}$, Kif3a$^{fl/fl}$, Ptch$^{+/-}$* mouse is tumorigenic. (**A**) MTT survival assay-derived cell growth ratio showing rapid proliferation of *Math1-Cre$^{ER}$, Kif3a$^{fl/fl}$* MB cell line relative to both fibroblast and colon carcinoma cell lines. Error bars depict ±SE. (**B**) *Math1-Cre$^{ER}$, Kif3a$^{fl/fl}$* MB cells form cilia under tumor ciliation protocol from Figure 3A. Percent ciliation is (number of cilia/number of nuclei) for each field and results depict quantification from three independent experiments. Percent ciliation of *Ptch$^{+/-}$* MB is also shown for comparison. Error bars depict ±SE. (**C**) Immunostaining (×40) showing *Math1-Cre$^{ER}$, Kif3a$^{fl/fl}$* MB cilia. Nuclei stained with DAPI (blue), cilia highlighted by acetylated tubulin (cyan). (**D**) *Math1-Cre$^{ER}$, Kif3a$^{fl/fl}$* MB cells exhibit anchorage-independent growth in soft agar assay. Bar graph depicts number of colonies >2 mm per ×10 field at 18 days after plating. Fibroblast cell line does not form colonies, but colon carcinoma and *Math1-Cre$^{ER}$, Kif3a$^{fl/fl}$* MB cells readily form colonies in soft agar. Error bars depict ±SE. (**E**) *Math1-Cre$^{ER}$, Kif3a$^{fl/fl}$* MB cells form heterotopic solid tumors when injected into the flank of nude mice. Tumor volume in cubic inches shown as a function of time (days) of

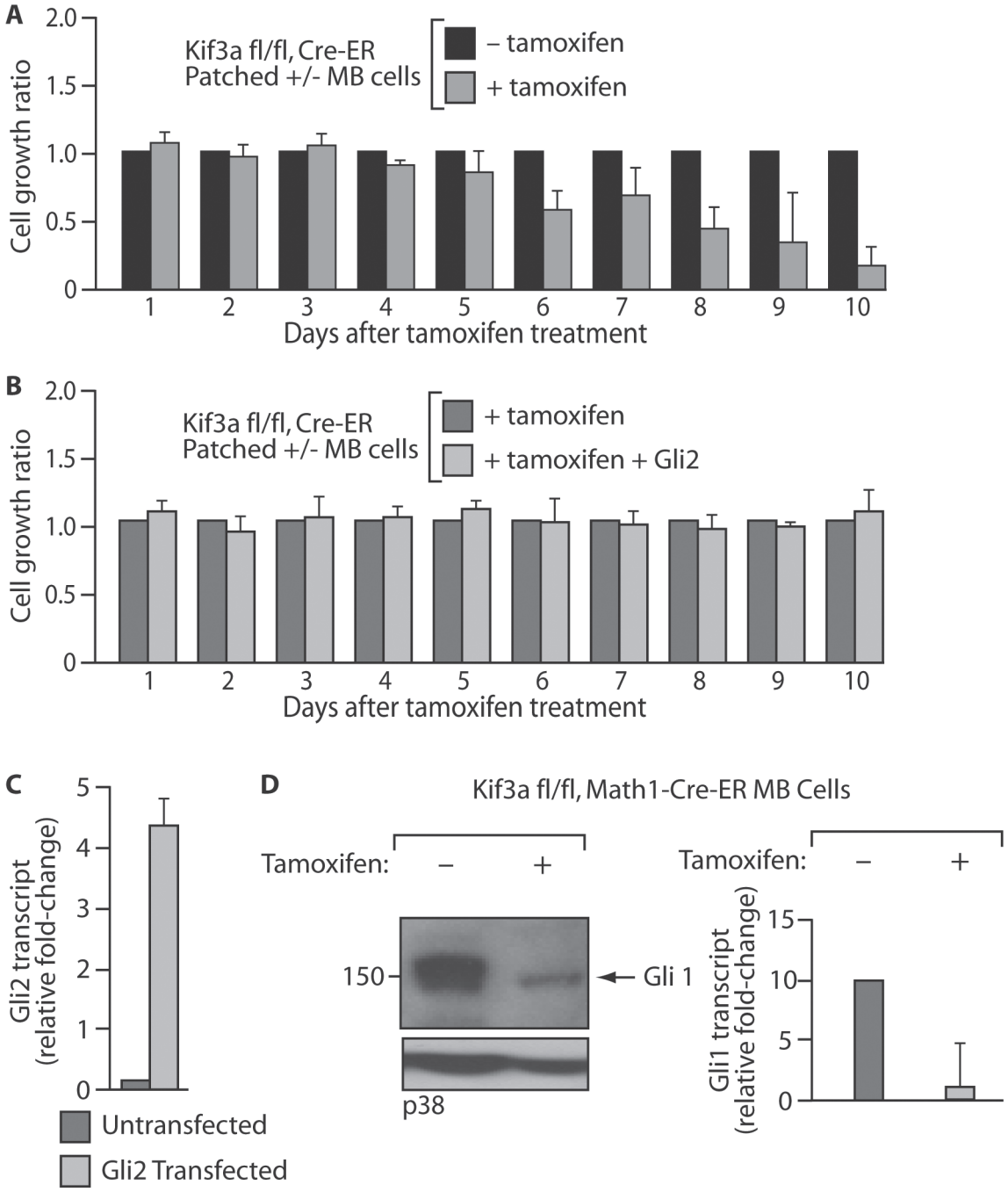


**Fig. 5.** MB cell line derived from *Math1-Cre*$^{ER}$, *Kif3a*$^{fl/fl}$, *Ptch*$^{+/-}$ mice requires KIF3a and cilia for cell survival and tumorigenesis. (**A**) Survival assay with tamoxifen treatment occurring on day 1. Loss of KIF3a results in death of *Math1-Cre*$^{ER}$, *Kif3a*$^{fl/fl}$ MB cells over a period that coincides with loss of KIF3a protein. Error bars depict ±SE. (**B**) Survival assay with tamoxifen treatment and transfection with *Gli2* occurring on day 1. Transfection of *Gli2* prevents cell death secondary to KIF3a loss in *Math1-Cre*$^{ER}$, *Kif3a*$^{fl/fl}$ MB cells. Error bars depict ±SE. (**C**) Quantitative PCR showing substantial increase in *Gli2* RNA levels in *Gli2* transfected versus untransfected cells. Error bars depict ±SE. (**D**) Protein blot 5 days after tamoxifen treatment showing reduced GLI1 levels as KIF3a protein levels decline. Quantitative PCR showing substantial decline in *Gli1* RNA levels 5 days after tamoxifen treatment. Error bars depict ±SE.

Cilia and *Kif3a* disruption specifically targeted to GNPs has not been reported prior to the present study. The precise roles of cilia in the developing cerebellum and in tumor cells remain a mystery, especially because MB cells have primary cilia only for the brief interval when they are not actively cycling. That appears to be time enough for the cilia to aid transduction processes, perhaps allowing

←
measurement after initial palpation of tumor. H&E image (×20) shows flank tumors with abundant cells with prominent nuclei in histological pattern consistent with MB. Error bars depict ±SE. (**F**) *Math1-Cre*$^{ER}$, *Kif3a*$^{fl/fl}$ MB cells injected into the cerebellum form solid tumors within 4–8 weeks. Left panel is a gross image of orthotopic tumor in central vermis region of cerebellum (encircled in red). Low power (×10, middle panel) shows infiltration of tumor cells within the cerebellum and high power (×30, far right panel) with line indicating the margin between normal cerebellum and MB. Tumor cells obliterate the left folium of the cerebellum (labeled MB) and a normal, organized cerebellum folium (labeled CB) is depicted on the right for comparison.

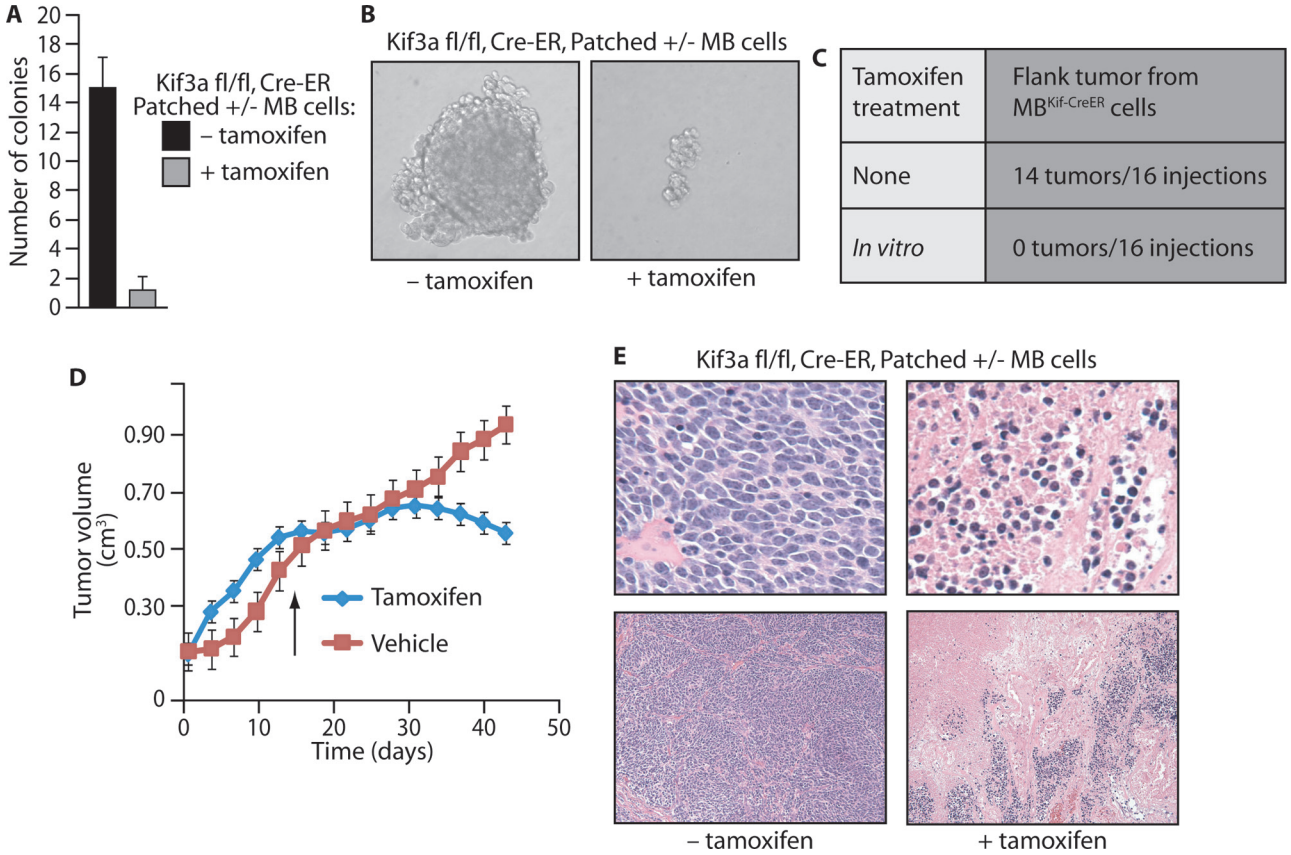


**Fig. 6.** Targeted deletion of *Kif3a* impairs tumorigenesis and causes tumor regression. (**A**) Soft agar assay showing impaired anchorage-independent growth of *Math1-Cre*$^{ER}$, *Kif3a*$^{fl/fl}$ MB cells after tamoxifen treatment. Tamoxifen treatment 10 days after colony formation resulted in scattered, sparse colonies that did not reach the 2 mm detection threshold on day 18. Error bars depict ±SE. (**B**) Brightfield image at ×60 (left) shows *Math1-Cre*$^{ER}$, *Kif3a*$^{fl/fl}$ MB cell colony 18 days after plating and (right) a small colony 18 days after plating and 8 days after tamoxifen treatment. (**C**) The number of tumors formed per injection of MB$^{Kif\text{-}CreER}$ cells tamoxifen-treated *in vitro* 1 day prior to injection into flanks and shoulders of immunodeficient mice. (**D**) Tumor growth curve with tumor volume (cubic inches) plotted against time (days tumor was measured after initial palpation). Error bars depict ±SE. Tamoxifen was administered beginning on day 15 (demarcated by black arrow). *Math1-Cre*$^{ER}$, *Kif3a*$^{fl/fl}$ MB flank and shoulder tumors stabilize then decrease in volume after tamoxifen treatment, whereas vehicle-treated mice show increased tumor growth volume over the same time period. (**E**) *Math1-Cre*$^{ER}$, *Kif3a*$^{fl/fl}$ MB cell flank and shoulder tumors in nude mice show characteristic MB histology (upper left, ×30) and high cellularity with prominent nuclei (lower left, ×15). After tamoxifen treatment, *Math1-Cre*$^{ER}$, *Kif3a*$^{fl/fl}$ MB tumors show enhanced fibrosis and necrosis (upper right, ×30). Tumor necrosis is prominent and characterized by focal hemorrhage, and karyorrhectic and pyknotic nuclear changes. A low-power image of tamoxifen-treated *Math1-Cre*$^{ER}$, *Kif3a*$^{fl/fl}$ MB tumors shows infiltrating inflammatory cells and diminished cellularity (lower right, ×15).

modification of Hh-transducing protein structures, associations, modifications or transport. Many Hh pathway-related functions have been proposed for cilia and the components of IFT that build cilia, but the precise role(s) of cilia in Hh signal transduction remains uncertain.

*Relationship of GLI proteins and KIF3a tested by epistasis*

GLI proteins mediate Hh pathway output, with GLI1 and GLI2 acting as transcriptional activators and GLI3 acting as an activator of transcription in its full-length form and a repressor of transcription in its processed form. With insufficient amounts of KIF3a, processing of GLI3 from its full-length activator form to its truncated repressor form is disrupted in fibroblasts (4,37,45,46). Loss of *Kif3a* prevents formation of cilia and blocks efficient formation of the repressor form of GLI3, resulting in constitutive low-level transcription of Hh target genes coupled with an inability to fully activate transcription of Hh target genes (Figure 2E).

In our experiments, introduction of additional GLI2 rescued the growth arrest of cultured *Kif3a*-deficient MB cells (Figure 5). Thus, enforced Hh pathway transcriptional activator expression is sufficient to overcome proliferation impairment caused by *Kif3a* deficiency. KIF3a localization and function is not limited to the cilium (47). If the main role of KIF3a in MB$^{Kif\text{-}CreER}$ cell growth was facilitation of intracellular trafficking or mitosis, GLI2 should not have been able to rescue proliferation in the cells. GLI2 is unlikely to repair the intracellular trafficking and mitotic deficits that occur upon *Kif3a* loss; a role for GLI2 in trafficking or mitosis has not been found. If KIF3a had an essential role in mitosis, we would expect cells lacking KIF3a to have mitotic and/or proliferation deficits. Fibroblasts lacking KIF3a (Figure 4) grew well, demonstrating that *Kif3a* is not essential for fibroblast proliferation or survival. KIF3a-deficient fibroblasts do not exhibit intracellular trafficking or mitosis defects (36) (data not shown). We conclude that the reason mutated *Kif3a* or an altered primary cilium affects tumorigenicity is because they are required for proper Hh target gene activation, not because of mitotic or intracellular transport defects.

MB cells and fibroblasts both require cilia for Hh target genes to be active despite the differences in how those genes are activated. MB cells have active SHH target genes due to loss of the target-repressing effect of PTCH receptor, a condition that obviates any need for a SHH signal. Nonetheless, cilia are required for the target genes to remain active. Fibroblasts turn on target genes in response to a SHH ligand, but cannot do so if they lack IFT components and cilia (Figure 4E) (48). The target genes in MB cells could in theory have remained active and capable of sustaining Hh pathway-driven tumor formation without any need for cilia. Our results and Han *et al.* (28). show the contrary: cilia are continuously necessary for proper SHH target gene

activation by GLI proteins in tumor cells. These findings are in accord with other studies that show the requirement for cilia in SHH target gene activation and repression. The role of cilia in target gene activation goes beyond early ligand reception steps.

*Ongoing growth of MBs depends upon continued function of Kif3a*

In humans, MB is diagnosed when it grows large enough to increase intracranial pressure and cause symptoms such as loss of balance, nausea, vomiting or headaches. The mouse model studies showing that KIF3a is necessary for MB initiation are not directly relevant to the already-formed MBs discovered in patients. We tested whether ongoing growth of MB depends upon continued function of KIF3a. By disrupting function of KIF3a in cultured MB cells and established tumors, we demonstrated that KIF3a, and likely cilia, is important for relentless tumor cell proliferation.

When *Kif3a* was disrupted in an established tumor, the tumor regressed over a period of time that mirrored the loss of KIF3a protein. This finding highlights the importance of KIF3a and cilia for Hh-driven tumor initiation and maintenance and may apply to other tumors that are initiated or sustained by unrestrained Hh signaling. The need to maintain Hh target gene function can evidently be fulfilled by the fleeting presence of cilia during periods between cell division. During this period, SMO may inactivate SUFU within cilia (10), unleashing activator forms of GLI proteins to enter the nucleus and stimulate transcription of target genes (49). The cilia may provide a scaffold and machinery conducive to production of GLI transcription factors that activate target genes and sustain MB proliferation. In tumor cells devoid of functional KIF3a, these events are no longer coordinated by the cilium and may occur haphazardly and less often. SHH target genes would never achieve maximal activation and the tumor's proliferative gene program and MB survival and tumorigenic potential would be impaired.

The results presented here highlight the importance of cilia in MB tumor formation and maintenance, and underscore the potential utility of cilium-disrupting agents for the treatment of other tumors that are addicted to the Hh pathway. The ciliopathies resulting from defective cilia involve many types of damage, including blindness, obesity and polycystic kidney disease. To develop a successful therapy against Hh pathway tumors, it would be valuable to identify components of cilia that, unlike KIF3a, are particularly important for Hh transduction but less so for other cilium functions.

## Supplementary material

Supplementary Figures 1–4 can be found online at http://carcin.oxfordjournals.org/

## Funding

National Science Foundation Graduate Research Fellowship (to M.T.B.); an American Association of Cancer Research Pancreas Cancer Action Network Fellowship, an Amgen Hematology-Oncology Fellowship and a Stanford University Developmental Cancer Research Award in Translational Science (to E.W.H.); Howard Hughes Medical Institute, a McDonnell Foundation grant and the National Institutes of Health (RO1 #18163 to M.P.S.).

## Acknowledgement

The authors wish to thank Drs R.Rohatgi and L.Milenkovic for *Kif3a*$^{fl/fl}$ *Math1*$^{Cre\text{-}ER}$ fibroblasts, Dr H.Vogel for neuropathological evaluation of MB, M.Masek for expertise in histology and immunohistochemistry and A.Grewall for expertise in histotechnology. We thank G.Schaaf for advice about MB cell line derivation, Dr C.C.Hui for the Gli2-Flag construct and Dr P.Beachy for PZP53 MB cells. We are further grateful to Drs L.Goldstein and J.Helms for *Kif3a*$^{fl/fl}$ mice, and Dr G.Fishell for *Math1-Cre*$^{ER}$ mice. We thank Drs J.-Y.Yang and E.Y.Lee for technical assistance and valuable advice, and Drs T.Stearns and M.Hayden for review and comments on the manuscript.

*Conflict of Interest Statement:* None declared.

## References

1. Hammerschmidt,M. *et al.* (1997) The world according to hedgehog. *Trends Genet*., **13**, 14–21.
2. Ingham,P.W. *et al.* (2001) Hedgehog signaling in animal development: paradigms and principles. *Genes Dev*., **15**, 3059–3087.
3. Evangelista,M. *et al.* (2006) The hedgehog signaling pathway in cancer. *Clin. Cancer Res*., **12**(20 Pt 1), 5924–5928.
4. Huangfu,D. *et al.* (2003) Hedgehog signalling in the mouse requires intraflagellar transport proteins. *Nature*, **426**, 83–87.
5. Rohatgi,R. *et al.* (2007) Patched1 regulates hedgehog signaling at the primary cilium. *Science*, **317**, 372–376.
6. Corbit,K.C. *et al.* (2005) Vertebrate Smoothened functions at the primary cilium. *Nature*, **437**, 1018–1021.
7. Haycraft,C.J. *et al.* (2005) Gli2 and Gli3 localize to cilia and require the intraflagellar transport protein polaris for processing and function. *PLoS Genet*., **1**, e53.
8. May,S.R. *et al.* (2005) Loss of the retrograde motor for IFT disrupts localization of Smo to cilia and prevents the expression of both activator and repressor functions of Gli. *Dev. Biol*., **287**, 378–389.
9. Chen,M.H. *et al.* (2009) Cilium-independent regulation of Gli protein function by Sufu in hedgehog signaling is evolutionarily conserved. *Genes Dev*., **23**, 1910–1928.
10. Jia,J. *et al.* (2009) Suppressor of fused inhibits mammalian hedgehog signaling in the absence of cilia. *Dev. Biol*., **330**, 452–460.
11. Goetz,S.C. *et al.* (2010) The primary cilium: a signalling centre during vertebrate development. *Nat. Rev. Genet*., **11**, 331–344.
12. Pan,J. *et al.* (2007) The primary cilium: keeper of the key to cell division. *Cell*, **129**, 1255–1257.
13. Scholey,J.M. (2008) Intraflagellar transport motors in cilia: moving along the cell's antenna. *J. Cell Biol*., **180**, 23–29.
14. Koyama,E. *et al.* (2007) Conditional Kif3a ablation causes abnormal hedgehog signaling topography, growth plate dysfunction, and excessive bone and cartilage formation during mouse skeletogenesis. *Development*, **134**, 2159–2169.
15. Altman,J. (1997) Early beginnings for adult brain pathology. *Trends Neurosci*., **20**, 143–144.
16. Wechsler-Reya,R.J. *et al.* (1999) Control of neuronal precursor proliferation in the cerebellum by Sonic hedgehog. *Neuron*, **22**, 103–114.
17. Wallace,V.A. (1999) Purkinje-cell-derived Sonic hedgehog regulates granule neuron precursor cell proliferation in the developing mouse cerebellum. *Curr. Biol*., **9**, 445–448.
18. Dahmane,N. *et al.* (2001) The Sonic hedgehog-Gli pathway regulates dorsal brain growth and tumorigenesis. *Development*, **128**, 5201–5212.
19. Northcott,P.A. *et al.* (2010) Genomics of medulloblastoma: from Giemsa-banding to next-generation sequencing in 20 years. *Neurosurg. Focus*, **28**, E6.
20. Hahn,H. *et al.* (1996) Mutations of the human homolog of Drosophila patched in the nevoid basal cell carcinoma syndrome. *Cell*, **85**, 841–851.
21. Johnson,R.L. *et al.* (1996) Human homolog of patched, a candidate gene for the basal cell nevus syndrome. *Science*, **272**, 1668–1671.
22. Goodrich,L.V. *et al.* (1997) Altered neural cell fates and medulloblastoma in mouse patched mutants. *Science*, **277**, 1109–1113.
23. Berman,D.M. *et al.* (2002) Medulloblastoma growth inhibition by hedgehog pathway blockade. *Science*, **297**, 1559–1561.
24. Schuller,U. *et al.* (2008) Acquisition of granule neuron precursor identity is a critical determinant of progenitor cell competence to form Shh-induced medulloblastoma. *Cancer Cell*, **14**, 123–134.
25. Spassky,N. *et al.* (2008) Primary cilia are required for cerebellar development and Shh-dependent expansion of progenitor pool. *Dev. Biol*., **317**, 246–259.
26. Chizhikov,V.V. *et al.* (2007) Cilia proteins control cerebellar morphogenesis by promoting expansion of the granule progenitor pool. *J. Neurosci*., **27**, 9780–9789.
27. Soejima,T. (1970) Fine structure of medulloblastoma. *Gann*, **61**, 17–26.
28. Han,Y.G. *et al.* (2009) Dual and opposing roles of primary cilia in medulloblastoma development. *Nat. Med*., **15**, 1062–1065.
29. Schaaf,G. *et al.* (2010) Silencing of SPRY1 triggers complete regression of rhabdomyosarcoma tumors carrying a mutated RAS gene. *Cancer Res*., **70**, 762–771.
30. Marszalek,J.R. *et al.* (1999) Situs inversus and embryonic ciliary morphogenesis defects in mouse mutants lacking the KIF3A subunit of kinesin-II. *Proc. Natl Acad. Sci. U.S.A*., **96**, 5043–5048.
31. Machold,R. *et al.* (2005) Math1 is expressed in temporally discrete pools of cerebellar rhombic-lip neural progenitors. *Neuron*, **48**, 17–24.
32. Chow,L.M. *et al.* (2006) Inducible Cre recombinase activity in mouse cerebellar granule cell precursors and inner ear hair cells. *Dev. Dyn*., **235**, 2991–2998.

33. Mosmann,T. (1983) Rapid colorimetric assay for cellular growth and survival: application to proliferation and cytotoxicity assays. *J. Immunol. Methods*, **65**, 55–63.
34. Helms,A.W. *et al.* (1998) Progenitors of dorsal commissural interneurons are defined by MATH1 expression. *Development*, **125**, 919–928.
35. Lumpkin,E.A. *et al.* (2003) Math1-driven GFP expression in the developing nervous system of transgenic mice. *Gene Expr. Patterns*, **3**, 389–395.
36. Corbit,K.C. *et al.* (2008) Kif3a constrains beta-catenin-dependent Wnt signalling through dual ciliary and non-ciliary mechanisms. *Nat. Cell Biol*., **10**, 70–76.
37. Huangfu,D. *et al.* (2005) Cilia and hedgehog responsiveness in the mouse. *Proc. Natl Acad. Sci. U.S.A*., **102**, 11325–11330.
38. Brattain,M.G. *et al.* (1980) Establishment of mouse colonic carcinoma cell lines with different metastatic properties. *Cancer Res*., **40**, 2142–2146.
39. Mo,R. *et al.* (1997) Specific and redundant functions of Gli2 and Gli3 zinc finger genes in skeletal patterning and development. *Development*, **124**, 113–123.
40. Corcoran,R.B. *et al.* (2001) A mouse model for medulloblastoma and basal cell nevus syndrome. *J. Neurooncol*., **53**, 307–318.
41. Yang,Z.J. *et al.* (2008) Medulloblastoma can be initiated by deletion of Patched in lineage-restricted progenitors or stem cells. *Cancer Cell*, **14**, 135–145.
42. Hatton,B.A. *et al.* (2008) The Smo/Smo model: hedgehog-induced medulloblastoma with 90% incidence and leptomeningeal spread. *Cancer Res*., **68**, 1768–1776.
43. Zhuo,L. *et al.* (2001) hGFAP-cre transgenic mice for manipulation of glial and neuronal function *in vivo*. *Genesis*, **31**, 85–94.
44. Wong,S.Y. *et al.* (2009) Primary cilia can both mediate and suppress hedgehog pathway-dependent tumorigenesis. *Nat. Med*., **15**, 1055–1061.
45. Liu,A. *et al.* (2005) Mouse intraflagellar transport proteins regulate both the activator and repressor functions of Gli transcription factors. *Development*, **132**, 3103–3111.
46. Humke,E.W. *et al.* (2010) The output of hedgehog signaling is controlled by the dynamic association between suppressor of fused and the Gli proteins. *Genes Dev*., **24**, 670–682.
47. Kondo,S. *et al.* (1994) KIF3A is a new microtubule-based anterograde motor in the nerve axon. *J. Cell Biol*., **125**, 1095–1107.
48. Ocbina,P.J. *et al.* (2008) Intraflagellar transport, cilia, and mammalian hedgehog signaling: analysis in mouse embryonic fibroblasts. *Dev. Dyn*., **237**, 2030–2038.
49. Ruiz i Altaba,A. (1999) Gli proteins encode context-dependent positive and negative functions: implications for development and disease. *Development*, **126**, 3205–3216.

*Received September 9, 2012; revised December 30, 2012; accepted January 29, 2013*